Trans-cis isomerisation of azobenzene amphiphiles containing a sulfonyl group

Stanisław Kucharski,[a]* Ryszard Janik,[a] Hubert Motschmann[b] and Christian Radüge[b]

[a] *Institute of Organic and Polymer Technology, Wrocław Technical University, 50-370 Wrocław, Poland. E-mail: kucharski@itots.ch.pwr.wroc.pl*
[b] *Max-Planck-Institute of Colloids and Interfaces, 12489 Berlin, Germany*

Received* (*in Strasbourg, France*) *15th February 1999, Accepted 22nd April 1999

Trans-cis isomerisation of the azo amphiphilic derivatives 4-(*N*-methyl-*N*-*n*-dodecyl)amino-4′-(*N*-thiazol-2-yl) sulfonamidoazobenzene (**1**) and 4-(*N*-methyl-*N*-*n*-dodecyl)amino-4′-(*N*-pyrimidin-2-yl)sulfonamidoazobenzene (**2**), each containing a sulfonyl group and a heterocyclic ring, was observed during irradiation of the amphiphile solutions at the absorption band maximum (*ca.* 450 nm). The reverse *cis-trans* transition occurred at room temperature as a thermal relaxation. Quantum chemical calculations yielded the optimum geometry of the *trans*, *cis* and transition forms. The *trans-cis* potential energy difference obtained by the DFT B3LYP method is in the range of 67.5–70.7 kJ mol^{-1} and the activation energy is *ca.* 129.7–132.5 kJ mol^{-1}, depending on the basis set. The UV-Vis spectra of the *cis* and *trans* form of **1** and **2** were calculated using the INDO1/S semiempirical program. The calculated spectra of the *cis-trans* mixtures and those obtained experimentally were very close in shape. For the alcanoyl derivative 4-(*n*-undecyl)carbonamido-4′- (*N*-thiazol-2-yl)sulfonamidoazobenzene (**3**) the illumination with low intensity monochromatic light (365 nm) caused isomerisation but the system needed up to 72 h to recover the *trans* form by thermal relaxation.

Isomerisation of azobenzene derivatives is one of the best known photoreactions. It has gained very broad attention because it can be applied to yield materials that are able to form photoreactive or photoresponsive systems.[1–4] The azobenzene derivatives are characterised by reversible transformations from the generally more stable *trans* form to the less stable *cis* form by irradiation (illumination) with UV or visible light. The reaction is reversible and back transformation from *cis* to *trans* can be achieved either by illumination (usually at a different wavelength) or by thermal relaxation. The light-induced changes in colour are also accompanied by changes in the refractive index, dielectric constant, dipole moment, *etc.*, all of which indicate the importance of the *trans-cis* isomerisation for various applications in linear and nonlinear optics. This also means that the reaction can be applied for optical data storage devices.

Many aspects of the isomerisation of azobenzenes have been studied. Much work was devoted to establish the reaction mechanism but still there is some uncertainty and rotation around the dihedral angle C–N=N–C or inversion of the C–N bond are still considered as possible.[2,5–9] The sensitivity of azo compounds to light has motivated the study of various materials containing the azo group to find eventual possibilities for practical applications. These materials were polymeric[10–20] and various amphiphilic compounds useful in Langmuir and Langmuir–Blodgett film formation[17–30] (including also polymers). The effect of illumination on the behaviour of the substances in various states of aggregation, shapes and forms has been studied. Investigations on the use of these materials for eventual data storage devices have also been carried out.[31–34]

The aim of our work was to study the isomerisation ability of unsymmetrical sulfonyl derivatives of azobenzene having the typical structure of amphiphilic compounds. We selected three amphiphiles having a hydrophobic hydrocarbon chain that contained 12 carbon atoms, as shown in Fig. 1. All of them have documented ability to form monolayer films and the chromophoric part of the molecules consists of a donor-acceptor electron system that makes them active as nonlinear optical materials.[35–37] The ability of the amphiphiles in question to undergo a *cis-trans* isomerisation was determined spectrophotometrically and accompanied by quantum chemical calculations. The geometry of the starting and transition structures was calculated at different levels of theory [semiempirical and *ab initio* RHF (restricted Hartree–Fock) and DFT (density functional theory)] to determine the energy of the reaction path. Additionally, the UV spectra of the *cis* and *trans* forms of the amphiphiles could be also calculated. This is rather important as normally it is very difficult to get the UV spectrum of the *cis* forms as they are usually unstable at room temperature and tend to undergo reverse *cis-trans* isomerisation.

Results and dicussion

The sulfonyl containing amphiphiles we studied are crystalline substances. They were expected to undergo the *trans-cis* isomerisation in a manner analogous to that of other representatives of the large azobenzene chemical family. The absorption

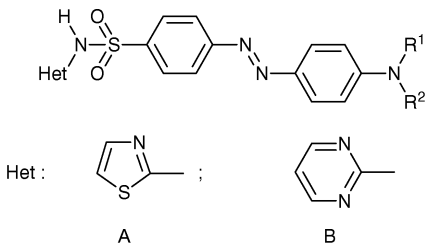

Compound	R^1	R^2	Het
1	CH_3	*n*-$C_{12}H_{25}$	A
2	CH_3	*n*-$C_{12}H_{25}$	B
3	H	*n*-$C_{11}H_{23}CO$	A

Fig. 1 Chemical formulas of the amphiphiles

spectra of their solutions recorded in the absence of external light showed similarities between compounds **1** and **2** with a maximum absorption peak appearing at *ca.* 448 and 454 nm, respectively. Derivative **3** showed an absorption peak at shorter wavelength, namely at 362 nm. The first two compounds have a structure with distinct electron donor and acceptor groups, the so called 'push-pull' electronic structure. The maximum absorption band is a broad peak that probably embraces the absorption ascribed either to n–π or π–π^* electron transitions. The presence of a carbonyl group, which is known to act as an electron acceptor, in close proximity to the alkyl amide nitrogen atom in **3** weakens the electron-donating ability of this atom. The shift of the maximum absorption band towards shorter wavelengths is caused by this effect. It should be mentioned that the alkyl amide nitrogen remains a net electron donor even if its close neighbour is the electron-withdrawing carbonyl group.[35,36]

Illumination of the chloroform solutions at a wavelength corresponding to the maximum absorption caused a photochemical reaction. Fig. 2 and 3 show the change in the absorption spectra of species **1** and **2** after illumination and thermal recovery at ambient temperature as a result of the reverse *cis-trans* isomerisation. Under analogous conditions compound **3** also underwent a photochemical reaction, seen as a decreasing maximum absorption peak but this reaction was not reversible and the spectrum of the illuminated sample remained unchanged with time, even if the sample was illuminated only 30 s. This means that illumination with the energetically stronger light beam obtained by passing light through WG335 and MG11 filters may be too intense and therefore destroy compound **3**. For this reason we decided to use the single 365 nm line of a Hg lamp (40 W) in a monochromator device. The illumination wavelength corresponded nearly exactly to the maximum absorption band of **3**. The chloroform solution was equilibrated in the dark for 48 h and while the light intensity was reduced the illumination time was prolonged. Fig. 4 shows the effect of illumination and the thermal recovery of the solution. The absorption band of **3** at *ca.* 265 nm increases its itensity after illumination but there is also a bulge at *ca.* 290 nm, which might indicate the presence of another absorption band. The band ascribed to n–π^* transition appears at *ca.* 450 nm, that is, in its usual place. It can be observed that the solution was not fully recovered at room temperature after 24 h. To achieve full *cis-trans* thermal recovery one has to wait up to 72 h.

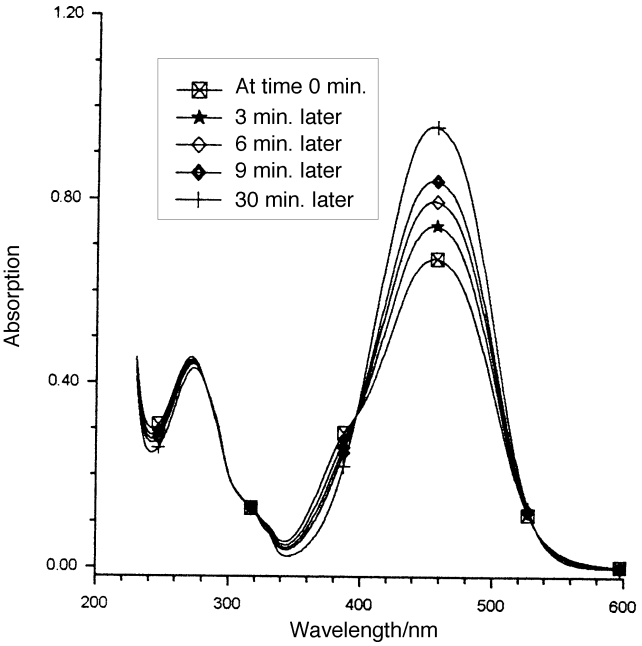

Fig. 3 *Trans-cis* isomerisation of **2**. Solution concentration: 1×10^{-4} mol dm^{-3}, cuvette: 1 mm.

1 and **2** showed some difference in their thermal recovery behaviour. The sulfathiazole derivative (**1**) undergoes some sort of side reaction during the illumination-recovery cycle and the compound does not recover the level of absorption that it had before illumination. Probably, we have to do with a partial loss of the substance due to an undesired side reaction. On the other hand, the sulfadiazine derivative (**2**) reacts reversibly without visible loss of material through 10 illumination-relaxation cycles.

Investigation of *trans-cis* isomerisation of azobenzene derivatives is in many instances troublesome as it is difficult to isolate the *cis* isomer in its pure form, which can then be preserved throughout the testing procedures. It is therefore difficult or even impossible to obtain experimental spectra of the

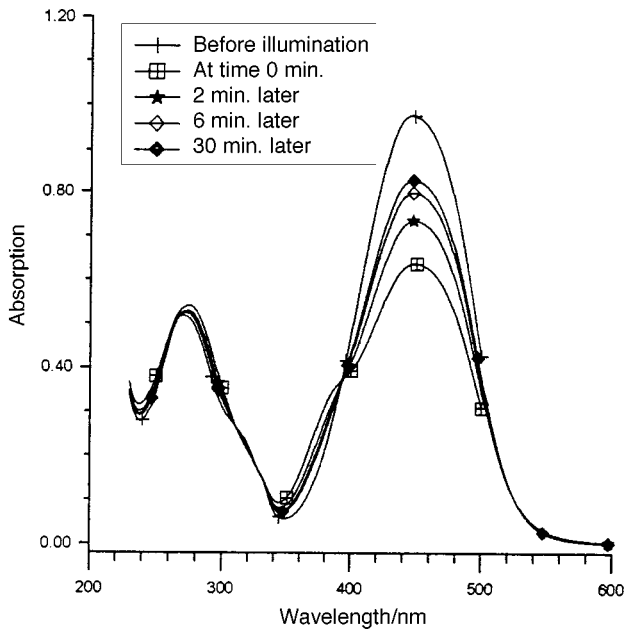

Fig. 2 *Trans-cis* isomerisation of **1**. Solution concentration: 1×10^{-4} mol dm^{-3}, cuvette: 1 mm.

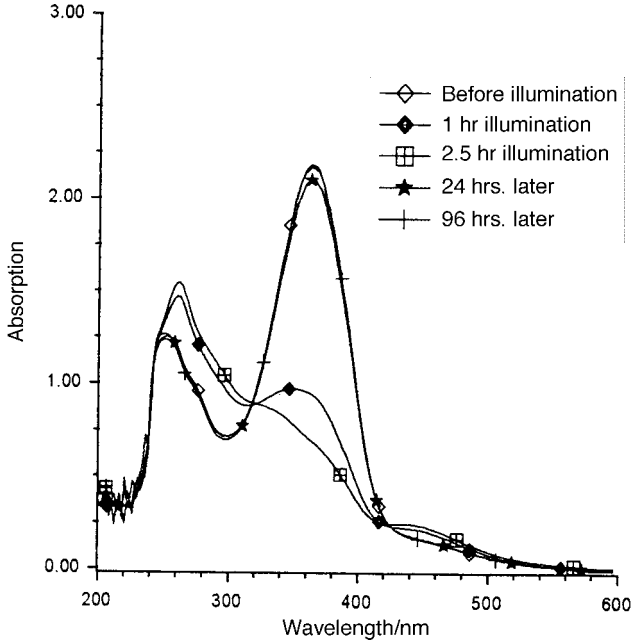

Fig. 4 Changes in the spectrum of compound **3** after illumination. Solution concentration: 6×10^{-6} mol dm^{-3}, cuvette: 10 mm.

cis form. There are, however, methods to overcome this problem if the spectrum of the *trans* form and that of a *cis*-*trans* mixture are available.[38,39] For the purposes of this work quantum chemical methods were applied at different levels of theory to determine the UV-Vis spectra of the *cis* isomers. We started with an optimisation of their geometrical structures using Gaussian 94. Several options such as PM3, RHF 3-21G (Hartree–Fock), B3LYP/3-21G and B3LYP/6-31G (DFT) were tested.

The structural parameters thus determined for the azo group and neighbouring atoms are given in Table 1. These are for amphiphile **1** and they are nearly the same for amphiphile **2**. According to the calculations, the fundamental changes during isomerisation are observed within three bonds connecting 4 atoms, marked 1, 2, 3, 4 in Fig. 5. The calculated bond lengths are different for various computational options. The DFT B3LYP/3-21G method yields a –N=N– bond length in the *trans* form equal to 0.13017 nm whereas DFT B3LYP/6-31G gives 0.12875 nm. Both values are much higher than that obtained experimentally by X-ray methods,[40–42] which was reported to be 0.1247 nm. The same experimental method used for *cis*-azobenzene gave a bond length equal to 0.1253 nm; the change of bond length during isomerisation was thus 0.0006 nm. A tendency to decrease the –N=N– bond length by *ca.* 0.002 nm when passing from the *trans* to *cis* form was indicated by all computational methods. The phenyl–azo–phenyl region of the *trans* isomer was planar, as indicated by the dihedral angle of nearly 180° found by all computational methods. In the *cis* form the dihedral C–N=N–C angle was between 0.1° (PM3) and *ca.* 11.3° for DFT methods.

Table 2 shows the analogous geometrical parameters around the azo group for compound **3**. Generally speaking, the geometry of the *trans*, *cis* and transition forms is analogous to those presented in Fig. 5, but the presence of the carbonyl group changes slightly the lengths of the bonds. Thus, the bond 3–4 which is closer to the alkyl amide group is longer by *ca.* 0.001 nm than the analogous bond of **1** or **2**. This involves also small changes in the length of bonds 1–2 and 2–3. The changes observed differ depending on the basis set applied in the geometry optimisation.

Using the semiempirical method PM3 the energy profile was obtained for passing from the *trans* to *cis* form by two reaction mechanisms. The first one was an inversion of the C–N=N (1–2–3) bond angle presented in Fig. 6(*a*) and the second one was the rotation around the dihedral angle C–N=N–C, shown in Fig. 6(*b*). The calculations were made by freezing the specific variable, either the bond angle or dihedral angle, enabling all other molecular parameters to be varied to find the global energy minimum. The energy profiles obtained for these two mechanisms are different in shape. Variation of the dihedral angle up to *ca.* 50° has only a small effect on the C–N=N bond angle but later on, the two variables seem to be

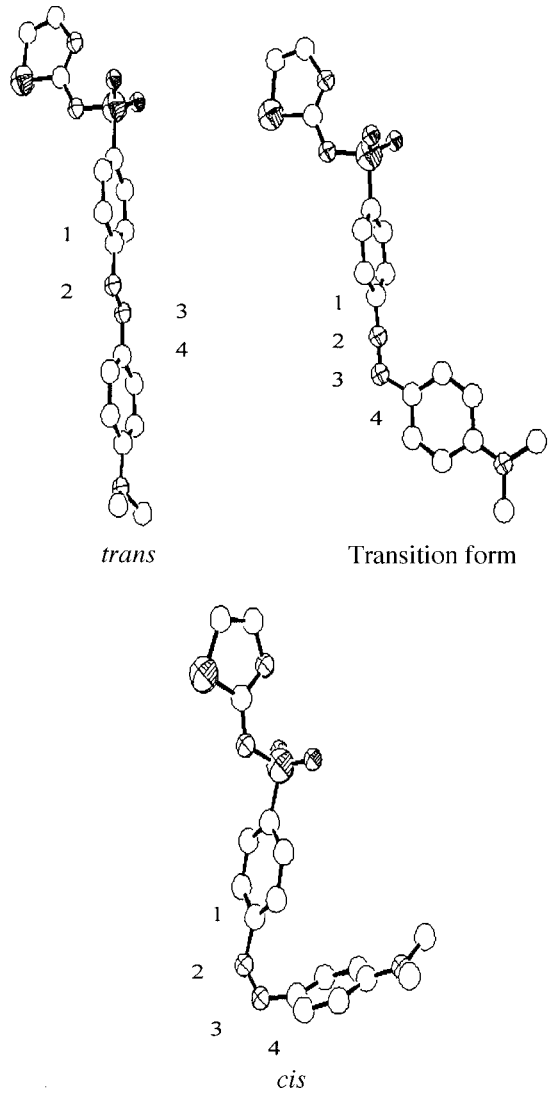

Fig. 5 Three-dimensional structures of **1** optimized by Gaussian B3LYP/3-21G option presented here for dimethyl derivative.

Table 1 Geometrical parameters around the azo group of the optimized geometry of the *trans*, *cis* and transition forms of **1**

	Bond length/nm × 10			Dihedral angle
Basis set	1–2	2–3	3–4	1–2–3–4/°
Trans form				
PM3	1.4494	1.2326	1.4397	179.9
RHF/3-21G	1.4255	1.2444	1.4075	179.8
B3LYP/3-21G	1.4245	1.3017	1.4007	179.9
B3LYP/6-31G	1.4221	1.2875	1.4001	179.8
Experimental*		1.247		
Cis form				
PM3	1.4502	1.2153	1.4523	0.1
RHF/3-21G	1.4348	1.2382	1.4287	6.1
B3LYP/3-21G	1.4351	1.2805	1.4242	11.3
B3LYP/6-31G	1.4307	1.2723	1.4213	11.3
Experimental*		1.253		8.0
Transition form				
PM3	1.3637	1.2119	1.4563	89.0
RHF/3-21G	1.3142	1.2140	1.4379	90.1
B3LYP/3-21G	1.3182	1.2465	1.4307	90.9
B3LYP/6-31G	1.3255	1.2439	1.4257	89.9

Table 2 Geometrical parameters around the azo group of the optimized geometry of the *trans*, *cis* and transition forms of **3**

	Bond length/nm × 10			Dihedral angle
Basis set	1–2	2–3	3–4	1–2–3–4/°
Trans form				
PM3	1.4483	1.2288	1.4483	179.7
RHF/3-21G	1.4272	1.2416	1.4157	179.9
B3LYP/3-21G	1.4283	1.2962	1.4123	179.8
B3LYP/6-31G	1.4195	1.2815	1.4106	179.7
Cis form				
PM3	1.4496	1.2160	1.4497	0.1
RHF/3-21G	1.4385	1.2363	1.4385	6.5
B3LYP/3-21G	1.4413	1.2755	1.4373	11.0
B3LYP/6-31G	1.4378	1.2693	1.4354	11.0
Transition form				
PM3	1.3654	1.2111	1.4595	89.2
RHF/3-21G	1.3185	1.2124	1.4483	89.6
B3LYP/3-21G	1.3184	1.2443	1.4568	89.7

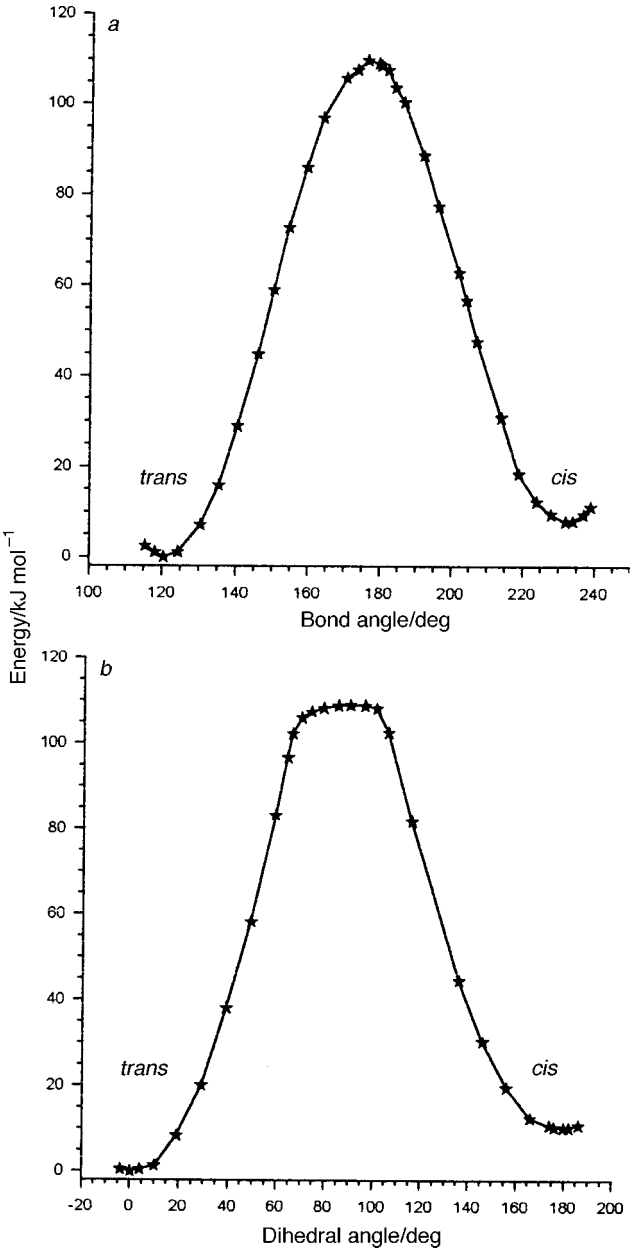

Fig. 6 Reaction energy path during isomerisation (*a*) by inversion and (*b*) by dihedral rotation.

interdependent, so that the change of the dihedral angle changes the molecular structure by increasing the 1–2–3 bond angle and thus causing its inversion. The switching in of the bond inversion is evidenced by the shape of the energy curve, which exhibits a plateau around the transition structure. At this point the 1–2–3 bond angle is nearly equal to 180°. In the case of the reaction path followed by inversion of the 1–2–3 bond angle the potential energy curve has the form of a peak. In this case the second mechanism of rotation around the dihedral angle starts closer to the transition point. The presence of the two contemporaneous mechanisms seem to be confirmed by the same value of the 'activation energy' from *trans* to *cis* forms, which is 109.7 kJ mol^{-1}. This does not confirm the results obtained years ago by the CNDO/2 method[43] but the energy values obtained by us are in the same range as reported earlier.[43,44]

It is regretful that the calculation of the reaction energy profiles could not be carried out by a more sophisticated *ab initio* method. Unfortunately, the duration of such calculations would make this enterprise rather costly, at least with today's technical possibilities. However, we managed to calculate energy levels for structures bordering the isomerisation path. The results obtained by 4 independent methods are tabulated in Table 3. The values of the energy barrier analogous to the activation energy of *trans-cis* isomerisation are reasonable and are in the range of reported experimental values cited by other authors. The difference of energy level for *trans* and *cis* forms is dependent on the calculation method. The most advanced DFT methods give values between 67.5 and 70.7 kJ mol^{-1}, which are in accord with experimental methods while the values yielded by PM3 and RHF/3-21G are far from the expected ones.

Looking at the structures shown in Fig. 5 one might notice that the sulfonamides could isomerise into other structures. Namely, the heterocyclic ring of the *cis* form is in the conformation relative to the *E* tertiary alkyl amine group, but the *Z* conformation would also be possible. Similar considerations might also be made concerning inversion. The transition structure shown in Fig. 5 indicates that the bond closer to the heterocyclic ring takes part in the reaction. Both questions were solved by calculation methods, which indicated that the models in Fig. 5 are energetically more favourable, although the gain of energy was in this case not significant.

To calculate the UV spectra of compounds **1** and **2** we introduced the atomic co-ordinates obtained by the most advanced B3LYP/6-31G option into the INDO1/S semi-empirical program.[45–47] The singlet state configuration interaction was assumed in the space from HOMO − 40 to LUMO + 40 that produced 1600 configurations. The effect of solvent was simulated by self-consistent reaction field (SCRF), using physical data for chloroform; the cavity radius of the solute in the solution was obtained from a Gaussian calculation. Twenty electronic states were generated which constitute a set of data: oscillator strength *vs.* energy of the excited state expressed in terms of frequency. This data was converted into a regular spectrum by applying a Gaussian envelope. For the *trans* forms of compounds **1** and **2** the first singlet excited state S1 generated by the program had a nearly zero value of the oscillator strength. The state S2 responsible for the π–π* charge transfer process was the dominant state with prevailing contribution of the HOMO–LUMO transition. The *cis* forms showed a stronger singlet state S1 at *ca.* 510 nm, which could eventually be seen as a small peak in the spectra but the charge transfer process π–π* ascribed to the HOMO–LUMO transition was less pronounced, as expressed by a reduced value of the oscillator strength.

In Figs. 7 and 8 the calculated spectra of **1** and **2** are shown. The spectra were obtained for the pure *trans* and *cis* forms and taking these as a base, the mixed spectra with up to 50%

Table 3 Potential energy levels of the isomerisation structures (*trans* isomer set at zero) obtained by calculation, in kJ mol^{-1}

	1		**2**		**3**	
Basis set	*Cis*	Transition	*Cis*	Transition	*Cis*	Transition
PM3	10.9	109.7	9.0	113.5	7.7	110.3
RHF/3-21G	81.7	157.9	81.5	159.9	81.3	161.3
B3LYP/3-21G	70.7	129.7	70.0	131.6	69.7	131.8
B3LYP/6-21G	67.5	131.6	67.4	132.5	—	—

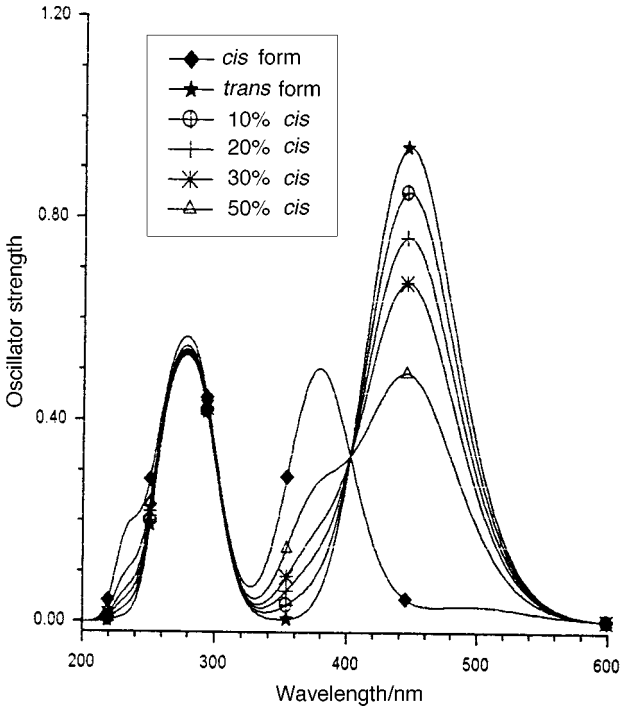

Fig. 7 The calculated UV-Vis spctra of **1**.

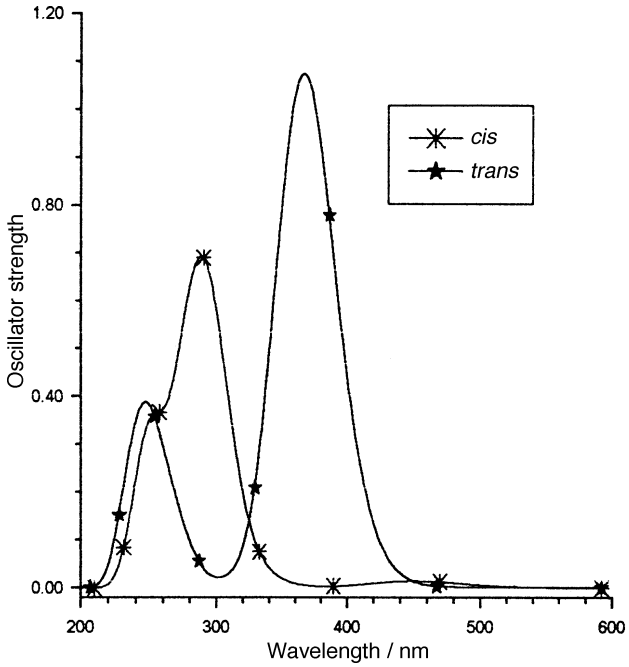

Fig. 9 The calculated UV-Vis spectra of **3**.

of the *cis* form were calculated. Comparison between experimental and calculated spectra lead to the conclusion that the agreement between the two pictures is very good. Moreover, by tuning the concentration of the amphiphile in the solution so as to obtain comparable peak heights of the *trans* form in experimental and in calculated spectra, one may evaluate the content of the *cis* form in illuminated solution by simply comparing the calculated and experimental spectra.

This procedure can hardly be recommended for compound **3**. The calculated spectrum of the *cis* form (Fig. 9) shows a strong absorption band at 288 nm, a second one at 255 nm and a weak band at 450 nm. The band at 255 nm is similar to that of the *trans* form. The illumination of the *trans* sample (see measured spectrum) causes a shift of the 255 nm absorption band to 265 nm and build-up of the band at *ca.* 286–8 nm. The latter two merge to form one band and its absorption intensity is *ca.* 70% that of the *trans* form. The shape of the measured spectrum cannot be generated by simple linear combination of the *cis* and *trans* spectra.

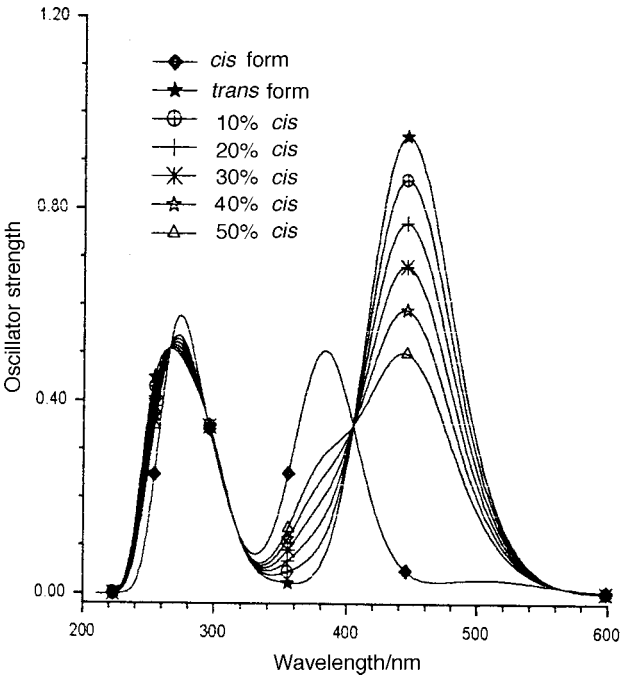

Fig. 8 The calculated UV-Vis spectra of **2**.

Conclusions

The azo sulfonyl amphiphiles containing a methyl alkylamine hydrophobic group (**1** and **2**) showed reversible isomerisation from the *trans* to *cis* forms when the amphiphile chloroform solutions were illuminated at a wavelength corresponding to the maximum absorption band. The reverse *cis-trans* isomerisation took place as a thermal relaxation reaction at room temperature. The sulfathiazole derivative **1** showed probable partial loss of the material (side reactions) during repeated illumination-relaxation cycle while the isomerisation of sulfadiazine derivative **2** was reversible during 10 cycles.

The quantum chemical calculations with the INDO1/S program resulted in simulated UV-Vis spectra of **1** and **2** in the *trans* form that were very similar to those obtained experimentally. The same procedure made it possible to generate the UV-Vis spectra of the *cis* forms and of the *trans-cis* mixtures containing up to 50 mol% of the *cis* form.

The alkyl amide derivative **3** undergoes *trans-cis* isomerisation under illumination but the thermal *cis-trans* recovery is very slow. To complete the reverse reaction a storage time of up to 72 h is required.

The calculated potential energy levels of the compounds in question using Gaussian DFT options yielded values of the *trans-cis* isomerisation energy which were in the range of 67.5–70.7 kJ mol^{-1}, close to the reported experimental values for isomerisation of azobenzene derivatives.

Experimental

General procedure for synthesis of 4-(*N*-Methyl-*N*-Alkyl)-amino-4′-(*N*-Heteroaryl)sulfonamidoazobenzenes

To a cooled below +5 °C solution of 0.015 mole sulfathiazole or sulfadiazine (Aldrich products) in mixture of 4.2 cm^3 (0.045 mole) concentrated HCl, 30 cm^3 water and 45 cm^3 glacial acetic acid, a solution of 1.2 g (0.0165 mole) $NaNO_2$ in 3 cm^3

water was added dropwise under stirring (reaction temperature was kept below +5 °C). After the reaction mixture was allowed to stand in ice water bath for 0.5 h an excess of sodium nitrite was decomposed by addition of a saturated water solution of sulfamic acid. To the solution of diazonium salt a cooled (0–5 °C) solution of 0.016 mole (*N*-methyl-*N*-alkyl)aniline in a mixture of 45 cm^3 glacial acetic acid and 4.5 cm^3 concentrated HCl was poured in; 15 g (0.18 mole) of anhydrous sodium acetate was then added and after stirring the reaction mixture allowed to stand overnight in a refrigerator. After dilution with a five-fold volume of water the coloured product was filtered off, washed with water, dried and crystallised from dioxane and/or a dioxane–water mixture.

4-(*N*-Methyl-*N*-*n*-dodecyl)amino-4′-(*N*-thiazol-2-yl)sulfonamidoazobenzene (1). Orange-red solid, yield 87%, mp 173–174 °C. ^{1}H NMR: 0.88 (t, 3H, CH_3C), 1.30 [m, 18H, $CH_3(CH_2)_9CH_2CH_2N$], 1.65 (m, 2H, $CH_2CH_2CH_2N$), 3.07 (s, 3H, CH_3N), 3.41 (t, 2H, $CH_2CH_2CH_2N$), 6.52 (d, $J = 4.6$ Hz, 1H, C=CHS of thiazole ring), 6.71 (d, 2H, *ortho* protons *vs.* NCH_3R of phenyl ring), 7.17 (d, $J = 4.6$ Hz, 1H, C=CHN of thiazole ring), 7.86 (d, 4H, *ortho* protons *vs.* –N=N– group of phenyl rings), 8.00 (d, 2H, *ortho* protons *vs.* $NHSO_2$ group of phenyl ring), 12.95 (br s, 1H, $NHSO_2$). IR (cm^{-1}): 645, 693 (ν_{SN}); 737 (γ_{CH}); 828, 845 (γ_{CHarom}; 857, 940 ($\gamma_{=CH}$); 1088, 1117, 1131 (δ_{CHarom}); 1156 ($\nu_{S=O}$, δ_{NH}); 1253 (ν_{CNarom}); 1294, 1328, 1379 ($\nu_{S=O}$); 1418, 1445, 1467 (δ_{CH}); 1517, 1540, 1575, 1582, 1601 ($\nu_{C=Carom}$); 2850 [ν_{CHsym} (CH_2)]; 2920 [ν_{CHas} (CH_2)]; 2953 [ν_{CHas} (CH_3)]; 3095 ($\nu_{=CHarom}$); 3140 (ν_{NH}). Anal. calcd for $C_{28}H_{39}N_5O_2S_2$: C 62.08, H 7.26, N 12.94, S 11.81; found: C 61.65, H 6.96, N 13.13, S 11.80.

4-(*N*-Methyl-*N*-*n*-dodecyl)amino-4′-(*N*-pyrimidin-2-yl)sulfonamidoazobenzene (2). Orange-red solid, yield 81%, mp 196.5–198 °C. ^{1}H NMR: 0.88 (t, 3H, CH_3C), 1.31 [m, 18H, $CH_3(CH_2)_9CH_2CH_2N$], 1.63 (m, 2H, $CH_2CH_2CH_2N$), 3.06 (s, 3H, CH_3N), 3.41 (t, 2H, $CH_2CH_2CH_2N$), 6.71 (d, 2H, *ortho* protons *vs.* NCH_3R of phenyl ring), 6.98 (t, $J = 4.7$ Hz, 1H, C=CHC of pyrimidine ring), 7.87 (dd, 4H, *ortho* protons *vs.* –N=N– group of phenyl rings), 8.20 (d, 2H, *ortho* protons *vs.* $NHSO_2$ group of phenyl ring), 8.67 (d, $J = 4.7$ Hz, 2H, NCH=CHN of pyrimidine ring), 11.92 (br s, 1H, $NHSO_2$). IR (cm^{-1}): 639, 669, 681, 691 (ν_{SN}); 730 (γ_{CH}); 730, 799, 827, 845, 942 (γ_{CHarom}); 1087, 1137 (δ_{CHarom}); 1167 (δ_{NH}, $\nu_{S=O}$); 1262 (ν_{CNarom}); 1315, 1344, 1378 ($\nu_{S=O}$); 1416, 1442 (δ_{CH}); 1493, 1519, 1582, 1602 ($\nu_{C=Carom}$); 2852 [ν_{CHsym} (CH_2)]; 2924 [ν_{CHas} (CH_2)]; 3038, 3084 ($\nu_{=CHarom}$); 3106 (ν_{NH}). Anal. calcd for $C_{29}H_{40}N_6O_2S$: C 64.89, H 7.52, N 15.67, S 5.96; found: C 64.77, H 7.55, N 15.87, S 5.81.

4-(*n*-Undecyl)carbonamido-4′-(*N*-thiazol-2-yl)sulfonamidoazobenzene (3). Its synthesis and spectral properties were described in ref. 48.

Methods

^{1}H NMR spectra were run on a 300 MHz Bruker Avance DRX-300 spectrometer for solutions in $CDCl_3$ and against TMS as internal standard. IR spectra were recorded on a Perkin–Elmer System 2000 FTIR spectrometer for KBr pellets. UV-Vis spectra were recorded in a Varian Cary 4E UV-Vis spectrophotometer.

Illumination of the chloroform solutions (*ca.* 10^{-4} mol dm^{-3}) was carried out using a mercury lamp and Schott glass filters: GG420 and BG28 for the light beam corresponding to the 450 nm absorption band (compounds **1** and **2**) and WG335 and MG11 for the absorption band of compound **3**. Additional experiments with the **3** solution were made using the 365 nm monochromatic band of a 40 W mercury lamp.

Quantum chemical calculations were carried out at the Wrocław Supercomputer Centre with an IBM R6000 RISC machine using GAUSSIAN 94 [49] and INDO1/S programs.

References

1 Z. Sekkat and W. Knoll, in *Advances in Photochemistry*, eds. D. C. Neckers, D. H. Volman and G. von Buenau, Wiley, Chichester, New York, Brisbane, Toronto, Singapore, 1997, vol. 22, pp. 117–195.
2 H. Rau, in *Photochemistry and Photophysics*, ed. J. F. Rabek, CRC Press, Boca Raton, 1990, vol. 2, pp. 119–141.
3 G. S. Kumar and D. C. Neckers, *Chem. Rev.*, 1989, **89**, 1915.
4 F. Voegtle, *Supramolecular Chemistry*, Wiley, New York, Chichester, Weinheim, Brisbane, Singapore, Toronto, 1993.
5 P. Bortolus and S. Monti, *J. Phys. Chem.*, 1979, **83**, 648.
6 S. Monti, E. Gardini, P. Bortolus and E. Amouyel, *Chem. Phys. Lett.*, 1981, **77**, 115.
7 I. K. Lednev, T.-Q. Ye, R. E. Hester and J. N. Moore, *J. Phys. Chem.*, 1996, **100**, 13338.
8 H. Rau and E. Lueddecke, *J. Am. Chem. Soc.*, 1982, **104**, 1616.
9 R. Takahara, T. Morozumi, H. Nakamura and M. Shimomura, *J. Phys. Chem. B*, 1997, **101**, 7736.
10 H. Menzel, *Makromol. Chem. Phys.*, 1994, **195**, 3757.
11 H. Menzel, J. S. McBride, B. Weicherst and M. Ruether, *Thin Solid Films*, 1996, **284–5**, 640.
12 J. Stumpe, T. Fischer and H. Menzel, *Macromolecules*, 1996, **29**, 2831.
13 J. Engelking and H. Menzel, *Thin Solid Films*, 1998, **327–9**, 90.
14 J. Gu, B. Liang, Y. Tian, Y. Chen, B. Lu and Z. Lu, *Thin Solid Films*, 1998, **327–9**, 427.
15 T. Seki, H. Sekigawa, S. Morino and K. Ichimura, *J. Phys. Chem. B*, 1998, **102**, 5313.
16 H. Tachibana, R. Azumi, M. Tanaka, M. Matsumoto, S. Sako, H. Sakai, M. Abe, Y. Kondo and N. Yoshino, *Thin Solid Films*, 1996, **284–5**, 73.
17 C. Tedeschi, M. Polli, M. P. Fontana and O. Pieroni, *Thin Solid Films*, 1996, **284–5**, 174.
18 J. Stumpe, L. Laesker, T. Fischer, M. Rutloh, S. Kostromin and R. Ruhman, *Thin Solid Films*, 1996, **284–5**, 252.
19 T. Seki, K. Ichimura, R. Fukuda and T. Tamaki, *Thin Solid Films*, 1996, **284–5**, 365.
20 J. Stumpe, T. Geue, T. Fisher and H. Menzel, *Thin Solid Films*, 1996, **284–5**, 606.
21 H. Tachibana, F. Sato, S. Terettaz, R. Azumi, T. Nakamura, H. Sakai, M. Abe and M. Matsumoto, *Thin Solid Films*, 1998, **327–9**, 813.
22 R. A. Moss and W. Jiang, *Langmuir*, 1997, **13**, 4498.
23 R. Wang, T. Iyoda, D. A. Tryk, K. Hashimoto and A. Fujishima, *Langmuir*, 1997, **13**, 4644.
24 R. Wang, L. Jiang, T. Iyoda, D. A. Tryk, K. Hashimoto and A. Fujishima, *Langmuir*, 1996, **12**, 2052.
25 R. A. Hall, M. Hara and W. Knoll, *Langmuir*, 1996, **12**, 2551.
26 K. Taniike, T. Matsumoto, T. Sato, Y. Ozaki, K. Nakashima and K. Iriyama, *J. Phys. Chem.*, 1996, **100**, 15508.
27 M. Schoenkopf, M. Mertersdorf and M. Loesche, *J. Phys. Chem.*, 1996, **100**, 7558.
28 T. Enomoto, H. Hagiwara, D. A. Tryk, Z.-F. Liu, K. Hashimoto and A. Fujishima, *J. Phys. Chem. B*, 1997, **101**, 7422.
29 T. Yamazaki, I. Yamazaki and A. Osuka, *J. Phys. Chem. B*, 1998, **101**, 7422.
30 Z. Sekkat, J. Wood, Y. Geerts and W. Knoll, *Langmuir*, 1996, **12**, 2976.
31 A. Natansohn, P. Rochon, J. Gosselin and S. Xie, *Macromolecules*, 1992, **25**, 2268.
32 A. Natansohn, R. Rochon, C. Barret and A. Hay, *Chem. Mater.*, 1995, **7**, 1612.
33 S. Xie, A. Natansohn and P. Rochon, *Chem. Mater.*, 1993, **5**, 403.
34 M. S. Ho, C. Barret, J. Paterson, M. Estehgamatian, A. Natansohn and P. Rochon, *Macromolecules*, 1996, **29**, 4613.
35 S. Kucharski, R. Janik and P. Kaatz, *J. Phys. Chem. B*, 1997, **101**, 8967.
36 S. Kucharski, R. Janik and P. Kaatz, *J. Mater. Chem.*, 1999, **9**, 395.
37 S. Kucharski, R. Janik, M. Bienkowski and J. Sworakowski, *Thin Solid Films*, 1998, **327–9**, 78.
38 E. Fischer, *J. Phys. Chem.*, 1967, **71**, 3704.
39 H. Rau, G. Greiner, G. Gauglitz and H. Meier, *J. Phys. Chem.*, 1990, **94**, 6523.
40 J. A. Bouwstra, A. Schouten and A. Kroon, *Acta Crystallogr., Sect. C*, 1977, **39**, 903.

41 M. Traetenberg, I. Hilmo and K. Hagen, *J. Mol. Struct*., 1977, **25**, 3561.
42 N. Biswas and S. Umpathy, *J. Phys. Chem. A*, 1997, **101**, 5555.
43 S. Ljunggren and G. Wettermark, *Acta Chem. Scand*., 1971, **25**, 1599.
44 E. V. Brown and G. R. Granneman, *J. Am. Chem. Soc*., 1975, **97**, 621.
45 M. A. Thompson and M. C. Zerner, *J. Am. Chem. Soc*., 1991, **113**, 8210.
46 M. A. Thompson, E. D. Glendening and D. Feller, *J. Phys. Chem*., 1994, **98**, 10465.
47 M. A. Thompson, *J. Phys. Chem*., 1996, **100**, 14492.
48 S. Kucharski and R. Janik, *Bull. Pol. Acad. Sci. Chem*., 1997, **45**, 319.
49 M. J. Frisch, G. W. Trucks, H. B. Schlegel, P. M. W. Gill, B. G. Johnson, M. A. Robb, J. R. Cheeseman, T. Keith, G. A. Petersson, J. A. Montgomery, K. Raghavachari, M. A. Al-Laham, V. G. Zakrzewski, J. V. Oritz, J. B. Foresman, J. Cioslowski, B. B. Stefanov, A. Nanayakkara, M. Challacombe, C. Y. Peng, P. Y. Ayala, W. Chen, M. W. Wong, J. L. Andres, E. S. Replogle, R. Gomperts, R. L. Martin, D. J. Fox, J. S. Binkley, D. J. Defrees, J. Baker, J. P. Stewart, M. Head-Gordon, C. Gonzalez and J. A. Pople, *Gaussian 94*, *Rev. D.2*, Gaussian, Inc., Pittsburgh PA, 1995.

Paper 9/01306G